Proceedings of the ASME 2010 3rd Joint US-European Fluids Engineering Summer Meeting and 8th International Conference on Nanochannels, Microchannels, and Minichannels
FEDSM-ICNMM2010
August 1-5, 2010, Montreal, Canada

FEDSM-ICNMM2010-31115

SIMULATION ON FLOW FIELD INDUCED BY VIBRATION SURFACE OF LOW FREQUENCY

Ling SHEN
Tel: +86-10-62794735, Fax: +86-10-62794735, E-mail: chenling08@mails.tsinghua.edu.cn
State Key Laboratory of Hydro science & Hydraulic Engineering, Department of Thermal Engineering
Tsinghua University, Beijing 100084, China

Shuhong LIU
State Key Laboratory of Hydro science & Hydraulic Engineering, Department of Thermal Engineering,
Tsinghua University, Beijing 100084, China

Yulin WU
State Key Laboratory of Hydro science & Hydraulic Engineering, Department of Thermal Engineering,
Tsinghua University, Beijing 100084, China

ABSTRACT

Ultrasonic cavitation generated by high-frequency ultrasonic transducer is widely studied because this phenomenon could be applied in a great variety of fields, including medical therapy, industrial cleaning as well as sewage treatment. Flow field influenced by vibration source of low frequency, however, is less studied. For the present study, a water tank of 1000×600×500mm is investigated when a vibration surface that represents a transducer of less frequency vibrates in the vicinity of one wall. Numerical computation based on the method of dynamic mesh is applied. Furthermore, two different vibration patterns are simulated, i.e., piston movement and drumhead vibration. Results show different pressure and velocity distribution within water tank when vibration surface is working at various frequencies and amplitudes. Differences of the flow fields are found between these circumstances, and similarity is found with that induced by ultrasonic transducer. Analysis on differences is discussed for further study.

Keywords: dynamic mesh, vibration boundary, flow field simulation

INTRODUCTION

Ultrasonic cavitation is a process of bubble formation, growth and collapse controlled by ultrasound. When the ultrasound travels in a liquid where there are naturally a great number of nuclei, the added pressure forces small cavities to grow in its positive phase and collapse in negative phase. The resultant high pressure and jet flow of bubbles could be applied both in fields of medical treatment and industry, thus, attracts attention of researchers worldwide.

Flow patterns induced by ultrasound, or rather, acoustic sources, have been studied by some researcher, mostly showing features of turbulence. Lighthill(1) explained in his work how turbulent jets called acoustic streaming are generated by sound, one that is forced by the action of a Reynolds stress. Acoustic streaming is a second-order phenomena if the amplitude of ultrasound becomes significantly large and the linear approximation does not hold any more (2).

A lot of simulations are done based on the wave equation or KZK equation in an attempt to get a flow field of various kinds. A numerical method was proposed for the simulation of acoustic fields, in presence of an obstacle in the physical domain, by finite difference solution of a two-dimensional differential model on boundary-fitted grids (3). The effect of ultrasound on flow through porous media has been investigated both experimentally and theoretically (4). Decrease in fluid viscosity is due to dissipation of acoustic waves and acoustic streaming. A three-dimensional numerical algorithm was developed to solve the KZK equation in the frequency domain for description of the asymmetrical nonlinear ultrasound field, and two kinds of rib configuration were used to simulation the typical situation in the therapeutic treatment of liver tissues (5). A simulation software based on a finite difference time domain three-dimensional scheme was developed to predict acoustic pressure in the brain during stroke treatment to help identify possible mechanism of intracerebral hemorrhage (6).

Note that the sound is actually generated by mechanical vibration (ultrasound with high frequency), which could be viewed as the basic physical model for simulation. Yet, there are few works on that. However, flow fields with moving boundary have been studied and could shed some lights on the methods of simulation. Musha and Kikuchi (7) presented a simplified simulation method for estimating the sonar self noise induced by hull vibration. Numerical solution of flow fields around a deformable cylinder body and vibrating string respectively in a duct was carried out by Satofuka and Nishitani using the rational Runge-Kutta scheme (8). The complex flow around standing breech was computed with large-scale moving boundaries (9). Local re-meshing method was applied to deal with grid-reforming of a high-speed bullet. Rincon and Rodrigues(10) obtained an approximated numerical solution for the model of vibrating elastic membranes with moving boundary. An extension of embedded-boundary formulations to laminar and turbulent flows interacting with moving boundaries on fixed Cartesian grids was investigated by Yang and Balaras(11), with systematic studies examining their accuracy and applicability in cases of moving boundaries.

In this paper, a method of dynamic mesh is adopted to simulate flow field of a water tank with a vibration surface placed near one wall representing low-frequency vibration source. Two different types of vibration are computed. Pressure and velocity distributions are presented for each case under different vibration amplitudes and frequencies. And variation of velocity with time in flow field is also shown in results. The results indicate that the method could be extended for simulation of high-frequency transducer to investigate ultrasonic cavitation. Given the fact that there is less research work concerning low-frequency transducer, this simulation is of value to some extent.

NOMENCLATURE

p = local static pressure

$\boldsymbol{v}$ = velocity vector t = time

Greek symbols

ρ = fluid density μ = viscosity

Subscripts

i, j, k = indices

NUMERICAL METHOD FOR SIMULATION

Physical modeling

The physical model for calculation is shown in Fig,1, where there is an open water tank with a hole on one side. The hole is for the placement of a piston acting as vibration source when it is driven by a motor to move back and forth along the hole. Model parameters are listed in Table 1.

Table 1 Model parameters

Water tank	1000×600×500 mm
The hole radius	50 mm
The hole length	50mm
Distance of hole center to the tank bottom	225mm
Fluid material	water at 25°C
Simulation type	unsteady

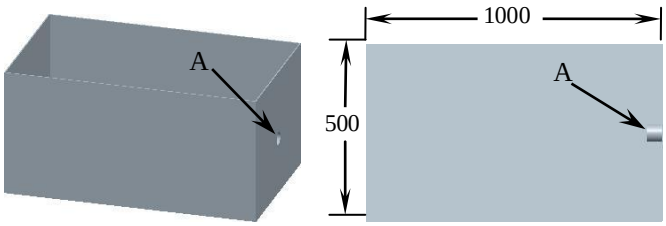

Fig.1 Physical model of the water tank

Governing equations in ALE

The water is treated as incompressible fluid which lead to the set of equations to be solved as

$$\frac{\partial \rho}{\partial t} + \nabla \cdot (\rho \boldsymbol{v}) = 0 \tag{1}$$

$$\frac{\partial \boldsymbol{v}}{\partial t} + (\boldsymbol{v} \cdot \nabla)\boldsymbol{v} = \frac{\mu}{\rho}\nabla^2 \boldsymbol{v} - \frac{\nabla p}{\rho} \tag{2}$$

Lagrangian or ALE methods are useful to handle problems with free or moving boundaries where the geometry in space changes with time. In such problems the space-time mesh may change continuously in time by letting the boundary nodes move according to specification and letting the internal nodes following in ALE using mesh smoothing, combined with occasional re-meshing with projection into the new mesh to avoid too strong mesh distortion.

The motion of a particle in Lagrangian coordinate $\boldsymbol{X}$ is described as

$$\boldsymbol{x} = \boldsymbol{x}(\boldsymbol{X}, t) \tag{3}$$

Whereas in Eulerian coordinate $\boldsymbol{x}$ as

$$\boldsymbol{X} = \boldsymbol{X}(\boldsymbol{x}, t) \tag{4}$$

In ALE, a reference domain Ω_χ is introduced which the grid is fixed with. So in this reference coordinate $o\chi_1\chi_2\chi_3$, the position of a particle is

$$\boldsymbol{\chi} = \boldsymbol{\chi}(\boldsymbol{X}, t) \tag{5}$$

Thus, the motion of a particle in this coordinate is

$$\boldsymbol{x} = \boldsymbol{x}(\boldsymbol{\chi}, t) \tag{6}$$

The velocities could be defined as

$$\boldsymbol{v} = \left.\frac{\partial \boldsymbol{x}(\boldsymbol{X},t)}{\partial t}\right|_{X} \tag{7}$$

$$\hat{\boldsymbol{v}} = \left.\frac{\partial \boldsymbol{x}(\boldsymbol{\chi},t)}{\partial t}\right|_{\chi} \tag{8}$$

$$\boldsymbol{w} = \left.\frac{\partial \boldsymbol{\chi}(\boldsymbol{X},t)}{\partial t}\right|_{X} \tag{9}$$

Note that $\hat{\boldsymbol{v}}$ is the velocity of grid node χ in Eulerian coordinate $\boldsymbol{x}$. The following relation could yield:

$$v_i = \hat{v}_i + \frac{\partial x_i(\chi,t)}{\partial \chi_j} w_j \tag{10}$$

And similarly, any physical property $F(\chi,t)$ can be expressed as

$$\left.\frac{\partial F}{\partial t}\right|_{X} = \left.\frac{\partial F(\chi,t)}{\partial t}\right|_{\chi} + c_i \frac{\partial F}{\partial x_i} \tag{11}$$

Based on (11), the governing equations using ALE in space domain Ω_x are written as

$$\frac{\partial v_i}{\partial x_i} = 0 \tag{12}$$

$$\frac{\partial v_i}{\partial t} + (v_j - \hat{v}_j)\frac{\partial v_i}{\partial x_j} = f_i - \frac{1}{\rho}\frac{\partial p}{\partial x_i} + \nu \frac{\partial^2 v_i}{\partial x_j \partial x_j} \tag{13}$$

Besides, geometrical conservation has to be satisfied as in $\frac{\mathrm{d}}{\mathrm{d}t}\int_V dV - \int_{\partial V} \boldsymbol{u_g} = 0$.

Boundary moving pattern

As mentioned above, two kinds of vibration pattern are engaged in calculation, i.e., piston movement and drumhead deformation. Specific codes have to be developed to achieve the goal of controlling dynamic mesh in desired manner.

During piston movement, the boundary is moving back and forth as a piston does, shown in Fig.2(a) where red dotted line represents the positions of moving wall. Fig.2(b) illustrates how the boundary is vibrating in drumhead manner during calculation, which is virtually a shape of parabola.

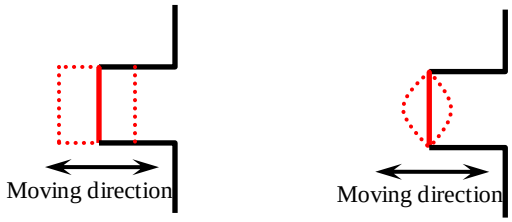

(a) Piston moving pattern **(b) Drumhead pattern**

Fig.2 Boundary moving pattern

Both patterns are controlled in sin function, i.e., $x = f(\boldsymbol{x})\cdot\sin(2\pi f \cdot t)$. The amplitudes and frequencies of vibration could be changed.

SIMULATION RESULTS

Considering the characteristics of dynamic mesh method and the frequencies set in simulation, the number of time steps in calculation has to be large enough to get a converged result. Moreover, VOF (Volume of Fluid) model is applied to calculate the free surface and no remarkable fluctuation of the free surface is observed which is what has been expected and desired.

Distributions with different amplitudes

In Fig.3, pressure distributions are listed with different vibrational amplitudes in piston movement. It is clear that basically the flow field is in similar pattern but tend to be more turbulent with higher amplitude reflected in the pressure range.

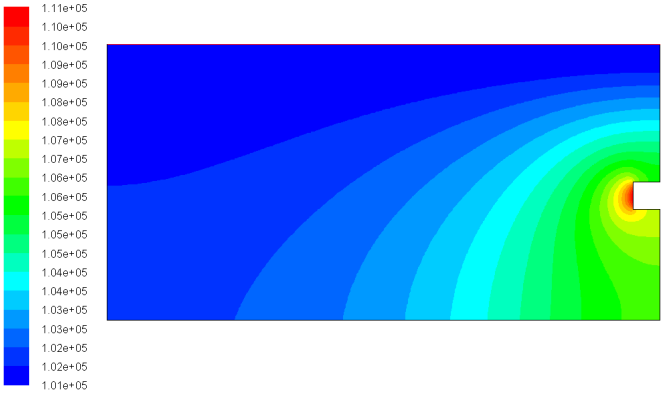

(a) 2mm, f=50Hz

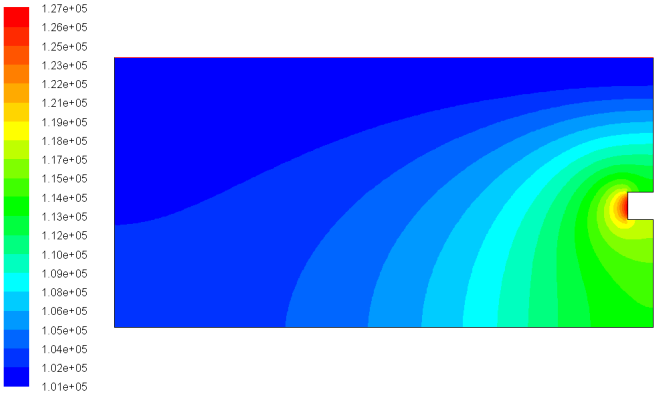

(b) 4mm, f=50Hz

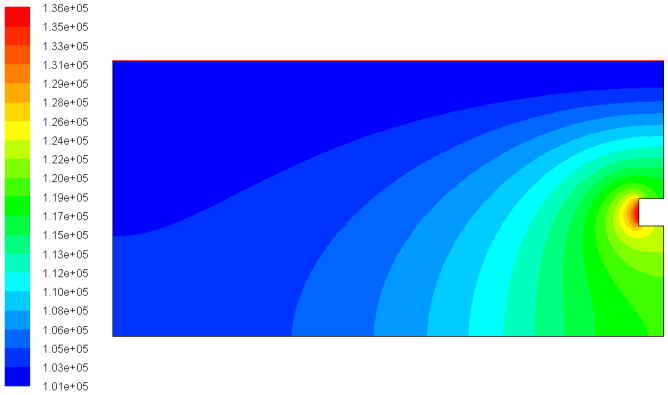

(c) 5mm, f=50Hz

Fig.3 Pressure distribution of flow field induced by piston movement with different amplitude at f=50Hz

Velocity distributions are displayed in Fig.4 with different vibration amplitudes in piston movement.

(a) 2mm, f=50Hz

(b) 4mm, f=50Hz

(c) 5mm, f=50Hz

Fig.4 Velocity distribution of flow field induced by piston movement with different amplitude at f=50Hz

The trend of turbulence can again be shown here, since values of velocity in Fig.4 (a), (b), (c) are basically increasing, and greater velocity gradient emerges around the moving boundary in (b) and (c). It is easy to understand, because greater amplitude means greater travelling distance of the piston, and more energy brought to the flow which transfers to fluid kinetic energy. Theoretical velocity value of fluid near moving wall could be calculated according to the velocity of moving wall which is programmed, and agreement between theoretical value and simulated one could validate dynamic mesh method to some extents.

Distributions with different frequencies

Comparison among distributions under conditions of different frequencies reveals the magnitude of impact vibration frequency has on flow filed.

Differences between Fig.3(a) and Fig.5(a) are apparent. When frequency of vibration boundary rises, the flow field evolves into a chaotic one. And the trend is also evident in velocity distribution, i.e., Fig.4(a) and Fig.5(b). In Fig.3(a), a regular layer-structure of the flow field forms, whereas in Fig.5(a) the kinetic energy seems to spread across whole field with irregular profile where a larger area of high pressure is presented. Higher frequency also brings about larger velocity value and thus more energy, because maximum velocity in Fig.5(b) is approximately 4 times of one in Fig.4(a).

(a) Pressure distribution

(b) Velocity distribution

Fig.5 Distributions of flow field induced by piston movement with 2mm amplitude at f=100Hz

Comparison between two vibration patterns

Comparison among distributions in different vibration patterns reveals a few features the moving boundary could bring to the fluid.

(a) Pressure distribution

(b) Velocity distribution

Fig.6 Distributions of flow field induced by drumhead vibration with 2mm amplitude at f=50Hz

The same amplitude and frequency of vibration wall, pressure field shown in Fig.3(a) exhibits large pressure gradient in the midst of field, while in Fig.6(a), large pressure gradient appears near the drumhead-vibrating boundary. This is probably because the piston movement disturbs more fluid than drumhead movement does, since it occupies more space during the vibration process.

Velocity fields of these two patterns indicate the same conclusion. Turbulence in Fig.4(a) can easily be seen, in particular around the piston. However, in Fig.6(b) with amplitude and frequency unchanged, regular arc-shaped velocity distribution is observed around moving boundary. It should be pointed out that velocity value right next to moving boundary in Fig.6(b) is also in agreement with theoretical value.

Fig.3(b) and Fig.7(a), Fig.4(b) and Fig.7(b) could be compared to yield similar result described above.

Actually, the drumhead vibration pattern is closer to the way that working surface of an ultrasonic transducer vibrates. Therefore, simulation of the flow field induced by an ultrasonic transducer might be viable by means of dynamic mesh.

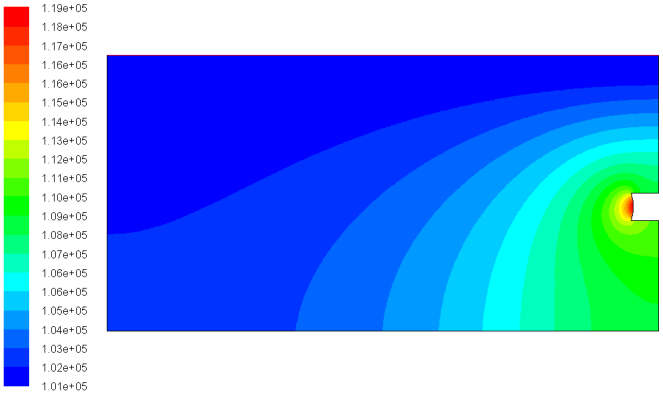

(a) Pressure distribution

(b) Velocity distribution

Fig.7 Distributions of flow field induced by drumhead vibration with 4mm amplitude at f=50Hz

Velocity variation with time

Considering the simulation is conducted as an unsteady one, velocity variation with time is also worth investigating. Shown in Fig.8 are 5 contours of velocity distribution near vibration boundary. As mentioned before, the wall vibrates sinusoidally, so 5 moments are chosen during a T=0.02s cycle with equal interval $\Delta t = 0.005s$. Positions of moving boundary in each figure could well illustrate the cycle.

The very first thing can be seen is periodicity of the velocity field, because Fig.8(a) and (e) are quite like not only in distribution but also in velocity value.

When velocity vector of the vibration boundary points toward the fluid, or to simply put, when the boundary is moving toward the internal flow field, there would form an arc-shaped profile with velocity distribution in layered structure, and maximum velocity emerges in a thin arc layer near wall (but not stick to the wall), seen in Fig.8(a)(c)(e). When the vector reverses, flow field changes accordingly-layered structure fades away, and maximum velocity exists at the corner of vibration wall, seen in Fig.8(b)(d).

These observation results are important because they might shed light on the mechanism of flow field induced by an actual ultrasonic transducer given the fact that there lies similarity in vibration patterns of the walls in two cases.

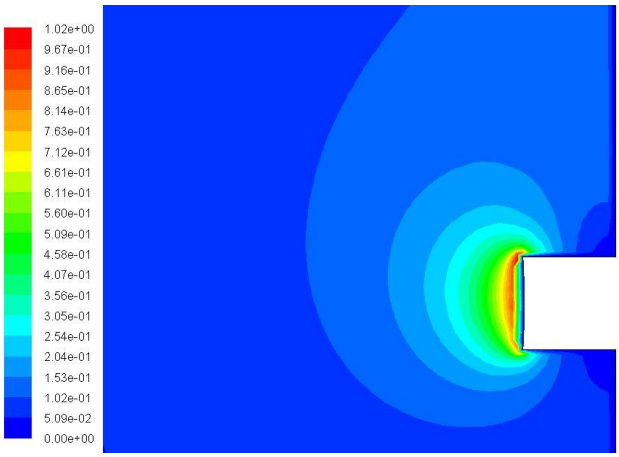

(a) t=1.0607s

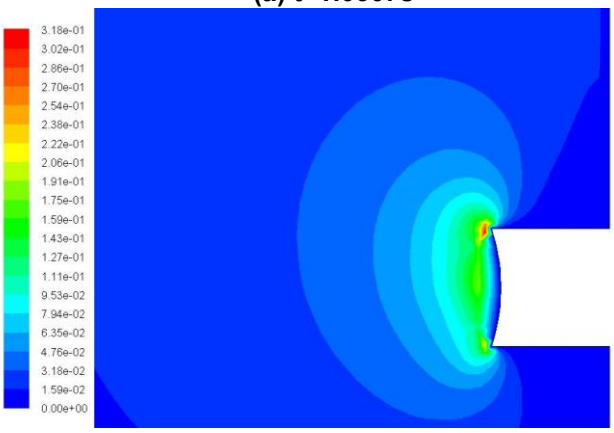

(b) t=1.0657s

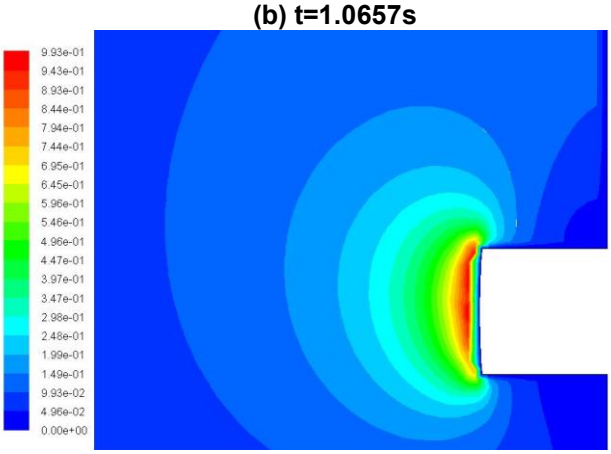

(c) t=1.0707s

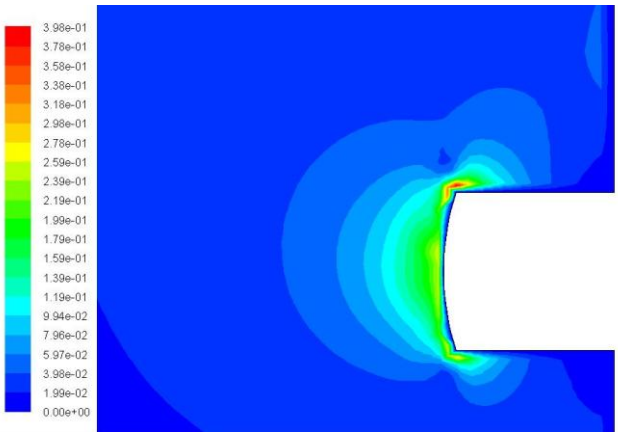

(d) t=1.0757s

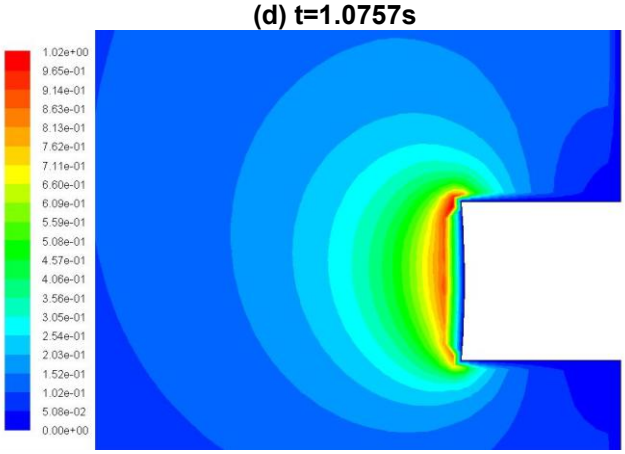

(e) t=1.0807s

Fig.8 Velocity variation within a vibration cycle T=0.02s (5 selected moments). The vibration pattern is drumhead type with 4mm amplitude, f=50Hz.

An experiment rig has been designed and would be established to conduct PIV test on the flow field same as one calculated above. The purpose of this measurement is to acquire characteristics of flow field induced by low-frequency vibration surface and to verify the calculating method of dynamic mesh. A water tank of 1000×600×500mm, as described above, is the testing object. The experimental results can be obtained, analyzed and compared with the simulation within a month or so to be further added into this research work.

CONCLUSIONS

1) Greater amplitude of the vibration boundary could induce a more chaotic flow field both in cases of piston movement and drumhead movement. It also contributes to a larger maximum velocity in the field.

2) Greater frequency of the vibration boundary could help to spread kinetic energy within the fluid. And it actually would bring more mechanical energy to the flow, creating a field with unique features. All the discussions are made under the circumstance of static free surface.

3) Provided with the same amplitude and frequency of vibration boundary, flow field generated by drumhead movement pattern is more stable, and velocity distribution is more concentrated around moving boundary. This pattern is similar to vibration from ultrasonic transducer (only an ultrasonic transducer is of much higher frequency to the magnitude of 10^5).

4) Dynamic mesh is proved in this paper to be a viable way to simulate flow field induced by vibration boundary of various types. As a result, further work on simulating and studying the field generated by acoustic transducer might be achieved this way.

5) Experimental data would be added into the existing simulated results for comparison and validation.

ACKNOWLEDGMENTS

The research is supported by the Chinese National Foundation of Natural Science (No. 50746022) as well as Open Foundation to State Key Laboratory of Hydro science & Hydraulic Engineering (SKLHSE-2010-E-01).

REFERENCES

1. Lighthill J. Acoustic Streaming. Journal of Sound and Vibration, 1978, 61(3): 391-418.

2. Wu J R, Wesley L. Nyborg, Ultrasound, Cavitation Bubbles and Their Interaction with Cells. Advanced Drug Delivery Reviews, 2008, 60: 1103-1116.

3. Cerimele M M, Pistella F, Spitaleri R M. Numerical Simulation of Acoustic Fields on Boundary-fitted Grids. Mathematics and Computers in Simulation, 2008, 79: 437-448.

4. Poesio P, Ooms G. Influence of high-frequency acoustic waves on the flow of a liquid through porous material. Proceedings on Physicochemical and Electromechanical Interactions in Porous Media, 2005: 61~66.

5. Li J L, et al. Influence of ribs on the nonlinear sound field of therapeutic ultrasound. Ultrasound in Med. & Biol., 2007, 33(9): 1413~1420.

6. Baron C, et al. Simulation of intracranial acoustic fields in clinical trials of sonothrombolysis. Ultrasound in Med. & Biol., 2009: 1~11.

7. Musha T, Kikuchi T. Numerical Calculation for Determining Sonar Self Noise Sources Due to Structural Vibration. Applied Acoustic, 1999, 58: 19-32.

8. Satofuka N, Nishitani T. Numerical Simulation of an Air Flow past a Moving Body with/without Deformation.

9. Wang B, Xu H Q. Simulation of Complex Flows with Large-scale Moving Boundaries. Chinese Journal of Computational Physics, 2008.7, 25(4): 396-400.

10. Rincon M A, Rodrigues R D. Numerical Solution for the Model of Vibrating Elastic Membrance with Moving Boundary. Communications in Nonlinear Science and Numerical Simulation, 2007, 12: 1089-1100.

11. Yang J M, Balaras E. An Embedded-boundary Formulation for Large-eddy Simulation of Turbulent Flows Interacting with Moving Boundaries. Journal of Computational Physics, 2006, 215: 12-40.